

## Article

# Unveiling the Complexity of Japanese Metallic Threads

Ludovico Geminiani <sup>1,\*</sup> , Francesco Paolo Campione <sup>2,3,4</sup>, Cristina Corti <sup>2,3</sup> , Sila Motella <sup>3,5,6</sup>, Laura Rampazzi <sup>2,3,7</sup> , Sandro Recchia <sup>1</sup>  and Moira Luraschi <sup>3,4</sup> 

- <sup>1</sup> Dipartimento di Scienza e Alta Tecnologia, Università degli Studi dell'Insubria, Via Valleggio 11, 22100 Como, Italy; sandro.recchia@uninsubria.it
- <sup>2</sup> Dipartimento di Scienze Umane e dell'Innovazione per il Territorio, Università degli Studi dell'Insubria, Via Sant'Abbondio 12, 22100 Como, Italy; francesco.campione@uninsubria.it (F.P.C.); cristina.corti@uninsubria.it (C.C.); laura.rampazzi@uninsubria.it (L.R.)
- <sup>3</sup> Centro Speciale di Scienze e Simbolica dei Beni Culturali, Università degli Studi dell'Insubria, Via Sant'Abbondio 12, 22100 Como, Italy; sila.motella@unicatt.it (S.M.); moira.luraschi@lugano.ch (M.L.)
- <sup>4</sup> Museo delle Culture, Villa Malpensata, Riva Antonio Caccia 5, 6900 Lugano, Switzerland
- <sup>5</sup> Dipartimento di Storia, Archeologia e Storia dell'Arte, Università Cattolica del Sacro Cuore, Largo Gemelli 1, 20123 Milano, Italy
- <sup>6</sup> Laboratorio di Archeobiologia, Musei Civici di Como, Piazza Medaglie d'Oro 1, 22100 Como, Italy
- <sup>7</sup> Istituto per le Scienze del Patrimonio Culturale, Consiglio Nazionale delle Ricerche (ISPC-CNR), Via Cozzi 53, 20125 Milano, Italy
- \* Correspondence: lgeminiani@uninsubria.it; Tel.: +39-031-238-6475

**Abstract:** In the framework of an extensive survey campaign on a collection of Japanese samurai armors, metallic threads from different parts of the traditional equipment were studied by several analytical techniques. The collection of armors belongs to Museo delle Culture (Lugano, Switzerland) and it is composed of ten elements, which date back from the 15th to 20th century. Metallic threads under study come from six of ten elements of the collection and represent a complex and unique multimaterial, which shows specific characteristics in Japanese tradition (*kinran*). The multianalytical approach based on ATR-FTIR spectroscopy and SEM-EDX analysis, together with a careful observation with optical and digital microscopy, permitted to obtain a complete characterization of materials, which have shown a great variability in metal foils and in organic adhesives (*urushi*, animal glue, starch). Gold and silver turned out to be not so largely used as scholars thought, while aluminum showed a great diffusion. Within the collection of analyzed armors, the obtained results allowed us for the first time to get a complete comprehension of materials and techniques used by Japanese craftsmen, and to observe differences in the quality of the materials and in manufacture technology over the centuries.

**Keywords:** japanese armor; metallic threads; *urushi*; *kinran*; ATR-FTIR; SEM-EDX



**Citation:** Geminiani, L.; Campione, F.P.; Corti, C.; Motella, S.; Rampazzi, L.; Recchia, S.; Luraschi, M. Unveiling the Complexity of Japanese Metallic Threads. *Heritage* **2021**, *4*, 4017–4039. <https://doi.org/10.3390/heritage4040221>

Academic Editors: Chiara Soffritti and Silvano Mignardi

Received: 31 August 2021

Accepted: 26 October 2021

Published: 28 October 2021

**Publisher's Note:** MDPI stays neutral with regard to jurisdictional claims in published maps and institutional affiliations.



**Copyright:** © 2021 by the authors. Licensee MDPI, Basel, Switzerland. This article is an open access article distributed under the terms and conditions of the Creative Commons Attribution (CC BY) license (<https://creativecommons.org/licenses/by/4.0/>).

## 1. Introduction

Metals have often represented a precious adornment for mankind since antiquity. Beyond jewelry and decorated metal artefacts for everyday life, metals in textiles deserve a particular mention. Depending on ages and cultures, clothes were decorated in various ways through patterned weaving, embroidery, painting, or dyeing; among these, the use of precious, metallic threads was generally considered distinctive and reserved to political and religious elites [1,2].

Many examples could be cited. Silver and gold wires are reported among Romans and Greeks [2–4], and gilded copper threads were found in an Egyptian coffin [5]. Actually, a well-documented diffusion in Europe of the use of metallic threads to decorate textiles started by the end of the first Millennium A.D. [1–3]. However, the majority of the studies concentrates on European production from the 13th to 17th century. Flemish Renaissance tapestries [6], Italian gentry' mantles [7], Hungarian [7] and Portuguese [8] liturgical vestments, and Greek/Byzantine ecclesiastical textiles [9] date back to this period. Successively,

the use of metallic threads did not decrease, and we can find it in Croatian liturgical vestments and festive folk costumes from the 17th to 20th century [10], Spanish coaches and furniture textiles from the 18th to 19th century [11], Turkish caftans and brocades dating between the 16th and 19th century [12], ornamentation for ecclesiastic clothing, religious statues, and church decoration from the Colonial Andes, which dates back to 17th and 19th century [13]. Pure gold, gold alloyed with silver, gilded or gilt-silvered copper, and gold-like copper alloys (e.g., pinchbeck alloy or brass) were used as the materials for the metal strips or wires [1], until the introduction of aluminum in the late 19th century, which brought to market new combinations of materials [14].

Karatzani [2] and J     [1] wrote a review about the historical development of the use of metal threads. Categories can be found based on their morphological characteristics:

- thin metal strips that were used either directly or, more often, wound around a fibrous core of silk, linen, cotton, or other yarns;
- gold or silver wire, which is wound creating a spiral, also known by the Turkish term *tir-tir*;
- gilt membrane strips: they were made by gilding leather, parchment, paper, or animal gut and then cutting the gilded material into strips. They were utilized in weaving and embroidery, either flat or wound around a fibrous core.

Both Karatzani and J     report that gilt membrane strips were the last to appear, beginning to spread over the Europe in the 11th or 12th century. The flexible thread eased the weaving process, it reduced the weight of clothing or fabric, and it decreased the cost. Initially, it was named “Cyprus gold threads” as it was imported from the East, from Byzantium or possibly from western Asian regions by ships through the port of Cyprus, or from North Africa across to southern European ports.

Actually, in Asia it was rather popular. English literature about the issue is extremely poor; it is generally referred that the development of gold thread embroidery originated in China, and that the technique spread to near countries [15,16]. As a matter of fact, an ancient brocade from the Metropolitan Museum of Art, which dates back to 13th century, is woven of silk and flat strips of leather membrane covered with gold leaf. According to the author, leather was generally substituted by a tough paper, successively [17].

In Japan [15,18,19], the first weaving technique imported from China was *nishiki*, which literally means “beautiful combination of colors”. This is a very colorful form of silk brocade with blue, red, yellow, purple, and other colored threads. The tradition dates back to the first example of Japanese-woven *nishiki* in the 5th century A.D. According to the story, Japanese students in the 11th century first brought from China a new form of brocade, the *kinran*. This was woven in characteristically Chinese patterns, with flat gold threads on a silk ground, and soon came to be much used by the Buddhist priests and nobles for vestments. In the *kinran*, the flat gold threads consist of a very fine tough paper made from the bark of the mulberry tree (*ko-zo*). Sheets of this *ko-zo* paper were spread with a thin preparation of lacquer and then with gold leaf, which was burnished on by hand and later cut into strips less than one millimeter wide. Thus was made the gold thread, which was woven into the *kinran* and which formed its characteristic feature. Actually, the most precious *kinran* continued to be imported from China until the beginning of 18th century. The increasing isolationist policy during the Edo period (1603–1868) gave initially a great improvement to the art of weaving in Japan, which was mainly located in the center of Sakai. However, in the last decades of the Edo period, a marked decadence in textile art occurred, contributed to by a Tokugawa government law that prohibited the selling of any silk brocades in order to put a limit to growing luxury and extravagance. Finally, the industrial fervor that Japan used to turn itself into one of the world’s most advanced nations nearly led to the extinction of ancient craft techniques [20], which were passed on by only a few individuals. Today in Japan, those who personify or singularly champions distinct craft practices are identified as “Holders of Intangible Cultural Property” and are more commonly recognized as “Living National Treasures” [21].

From ancient times in Japan, textiles like *nishiki* and *kinran* occupied a secure position in the hierarchy of the arts and crafts and have never been considered inferior to painting

or sculpture [16]. Todaiji Shosoin (Imperial Treasure Repository) in Nara contains many textiles, and items such as priest robes worn by high-ranking Buddhist monks have been passed down from generation to generation in the temples. In addition, they contain an abundance of fine kimono from the early modern period worn by aristocrats, the warrior class, and commoners. In the same way, shrines contain also the most precious *yoroi*, which is ancient-fashioned samurai armor, which date from the 12th to the second half of the 15th century [22]. In the 18th century, these original *yoroi* and later *gosoku*—the “modern armor” realized during the Age of Battles (1467–1613)—were considered by scholars [23] the best reference of constructive quality and functionality. Nevertheless, during the Edo period (1603–1868), samurai were better off than they had ever been and their prosperity is reflected in the enrichment of their arms and armors, which become mainly ceremonial uniforms [22]. Gold threads and precious brocades, as well as wide golden gilt surfaces, started to be used more and more frequently to create magnificent armors that showed off a samurai’s power. Different craftsmen’s work was blended by *saihoshi*—a kind of *ante litteram* stylist—in order to obtain an artefact that was intended to blend aesthetic value with the shape of traditional armor [23].

Actually, Japanese armor differs from European models mainly by the extensive use of textiles and Japanese lacquer (*urushi*). They both had a practical and an aesthetic reason considered essential in the manufacture of the armor. *Urushi* is a natural polymeric material, which was applied on the surface of metallic plates that constituted the core of the armor, offering protection from oxidation and extra-strength against blades. On the contrary, textiles were used both for the lacing (*odoshi-ge*) that joins metal plates together and for internal linings and paddings. Strongly colored dyed silk was preferred for the lacing, while for linings precious brocade fabrics as well as raw cotton or hemp linen were used. *Nishiki* and *kinran* were broadly used to decorate textiles, both in brocades and with embroidered details. Finally, various parts made with dyed or printed leather completed the armor, which appeared profusely colored. Every clan had its own colors that represented it through a combination of dyes chosen for the armor [23].

The state-of-the-art analysis on historical metal threads is rich due to the diffusion of this kind of artefact over many countries and ages. Some authors concentrate on material identification for conservation purposes, some on technological issues about gilding manufacture, others on degradation products. Even if some innovative approaches have to be mentioned [3–5,7,24–26], the majority of works relies on routinely and well-tested techniques. First of all, optical microscopy (OM) and scanning electron microscopy (SEM) are fundamental for a preliminary analysis of the sample dimension, morphology, and surface [1,5–9,13,14,27,28]. For example, degradation and corrosion of layers can be appreciated [12,13,29], as well as information about the manufacturing techniques [1,7,13,27,29,30]. Successively, X-rays techniques such as XPS [26,29], XRF [10,13,31], and EDX [5–10,13,14,24,27,28,31,32] are the most common ways to have a characterization of the metallic part, the last permitting also to obtain elemental maps, which are useful to appreciate dislocation of degradation products [8,11]. Also, X-ray diffraction (XRD) is seldom used to characterize materials adhering to the metal strips [31] or degradation products on the surface [11,13]. Nevertheless, a problem reported by Costa [32] is that surface analysis with EDX does not allow to catch the complexity of the stratigraphy, as it emerged that metal cores were often gilded with a more precious metal such as gold. A way to overcome the problem was suggested by Tronner [26] in 2002 and recently proposed again by Oraltay, as a cross-section approach is obviously very informative, but time and sample consuming [12]. It consists in performing measurements at different voltages to detect the composition at different depths [12,27]. The preparation of a polished cross-section for this kind of sample is a diffused practice, anyway [8,9,13,14,32]. Other ways to conduct a line profile analysis are using a dedicated XRD instrument [3] or preparing polished cross-sections by focused ion beam milling, which were successively analyzed with traditional techniques [7]. Also, scanning Auger microprobe (SAM) is based on a similar principle, using emitted low energy Auger electrons [26].

In some cases, other elemental techniques have been associated with EDX to get a more accurate quantification with lower limits of detection; some examples are SIMS [6,29], EPMA-WDS [7,9], ICP-OES [33], AAS [34], but all these techniques are reported to be destructive for the sample and they cannot differentiate between the surface and the core.

Further to the metallic parts, also organic components and decay products have been objects of studies, even if the literature is not equally rich. Morphology tests carried out by optical microscopy and scanning electron microscopy are generally the most common way to get information about the fiber core when metallic threads are wrapped around textiles [8,13,24,27,30,33,34]. An alternative way to get information from the organic yarns is to use thermogravimetric analysis [24] or XRD [11]. When the presence of other materials is presumed, spectroscopic techniques are used to get a complete characterization of organic materials such as lacquers, varnishes, and glues or inorganic degradation products. FTIR [11,13,14,24,34] or micro-Raman spectroscopy [7,11] have been extensively used for this purpose. SEM-EDX or XRF is also a diffused technique to investigate the organic support when it shows inorganic fillers and mordants [8,13,35], which appear frequently on gilt paper samples.

The present study dealing with six samples is part of a wider characterization project of most materials coming from the whole armor collection, whose results will be discussed in future articles. A wide variety of materials was sampled so as not to create visible damage to the artworks and many threads from each armor were analyzed within the analytical campaign. In this article, we present and discuss the analysis of only those with a metallic part. Thus, the aim of the current research work is to investigate on materials and manufacturing techniques used for the metallic threads that appear in the collection, in order to increase our knowledge about this particular collection and to give some useful indications for a wider study about *kinran*. To the best of our knowledge, no scientific investigation on such Japanese artefacts is reported in the scientific literature. Some non-English literature can be found, anyway, specifically in Korean [36,37]. Thus, this article intends to be the first filling a gap in the knowledge about this kind of applied art. Hence, our choice to use a well-tested analytical protocol, conducted on a selection of micro-samples. After a preliminary morphologic observation with OM and SEM, SEM-EDX was chosen for elemental analysis (which gives the possibility to obtain elemental maps), and ATR-FTIR spectroscopy for the recognition of organic and inorganic materials. As literature search highlighted the gilding thickness problem, metallic thread samples were successively embedded in epoxy resin to obtain polished cross-sections, which were successively analyzed with SEM-EDX.

This combination of analytical techniques enabled analysis of the composition and types of the metal threads, and the identification of the organic part. Our results brought new information about the set of armors that the threads belong to and shed new light on a chapter of Japanese applied art history.

## 2. Materials and Methods

### 2.1. The Morigi Collection

Nine Japanese full armors and a set made by a helmet (*kabuto*) and a mask (*menpō*) are from the Morigi Collection, donated to the Museo delle Culture Lugano (MUSEC) in 2017. Paolo Morigi, the collector, who already owned one Japanese armor (2017.Mor.4), acquired all the others in two auctions held in Nice and Paris in June 2016. The collection was presented in a temporary exhibition at the MUSEC in 2018 and is now currently shown there.

The collection shows different styles and dates of Japanese armor. In the absence of historical documents certifying a confident dating, experts suggested a dating on the basis of both a visual inspection and a stylistic analysis. All information about the collection is contained in the temporary exhibition catalogue [38].

All the armors are *kinsei gusoku* ("modern time armor") made in the Azuchi-Momoyama period, the harshest period of feudal wars in Japan spanning for all the second half of



the 16th century, or in the peaceful Edo period (1603–1868) or even later, in the Meiji (1868–1912), Taishō (1912–1926), and Shōwa period (1926–1989) up to the Thirties.

Armour 2017.Mor.7 is a battle armor of the Azuchi-Momoyama period, made to be tested in the battlefield, so it is anatomically shaped, particularly light-weight, and comfortable to wear.

The other armors were made when armors were used for celebrations and parades only. Some of them still have some war-tested elements made in the previous period, for example, the helmet (*kabuto*) of 2017.Mor.3, as well as his greaves (*suneate*).

Armour 2017.Mor.4 and 2017.Mor.9 are *kinsei gusoku* made according to the old-fashioned style (*mukashi gusoku*, «once upon a time armor») used in the Middle Age. Six samples from the above mentioned armors are the object of this study and are listed in Table 1 and shown in Figure 1.

## 2.2. Sampling

During sampling, we took care to balance sampling representativeness and the necessity to respect the artefacts. In the present case, the widest variety of materials was sampled paying attention not to create a visible damage. To assure the best representativeness, we made use of digital microscopy during the sampling to pay particular attention to the homogeneity of the sample and to the fact that no discrepancies were evident between the aspect of the analyzed material and the suggested dating.

The thread samples, generally only a few millimeters long, were taken under the condition of not causing visible damage to the artefact, i.e., from previously damaged areas or in hidden places.

The samples were collected using scissors and tweezers and stored in LDPE containers until analysis in the laboratory.

## 2.3. Polished Cross-Sections Preparation

Micro-fragments of samples were embedded in an epoxy resin, cross-cut with a diamond saw, and then mechanically polished. Particular care was taken not to use up entirely the sample taken from the armor.

## 2.4. Optical Microscopy

The textiles from which the samples were taken were observed in situ with a portable digital microscope MAOZUA USB001 (Mustech Electronics Co., Ltd., Shenzhen, China) and images were acquired using the software MicroCapture Plus, version 3.1.

The thread samples were then observed in the laboratory with an optical microscope Nikon Eclipse LV150 (Nikon Corporation, Tokyo, Japan), equipped with a Nikon DS-FI1 digital image acquisition system. Images were acquired and elaborated using the NIS-elements F software, version 3.22. Polished cross-sections were also observed, both in dark and in bright field mode.

**Table 1.** Description of the samples from the Morigi Collection. The position in the armor and the supposed dating for each sample are shown.

Sample	Description	Armor Element	Position Details	Armor Supposed Dating
3_6	Golden wire from textile	Vambrace ( <i>kote</i> )	External brocade lining	Early 17th century
4_7	Grey wire from textile	Vambrace ( <i>kote</i> )	External brocade lining	Mid-18th century
5_2	Silver-colored wire from textile	Helmet ( <i>kabuto</i> )	Helmet lace	Early 20th century
6_1	Golden wire from textile	Belt ( <i>iwa-obi</i> )	Brocade lining	Early 20th century
7_5	Golden wire from textile	Vambrace ( <i>kote</i> )	Internal brocade lining	Late 16th century
9_7	Golden wire from textile	Belt ( <i>iwa-obi</i> )	Brocade lining	Late 19th century

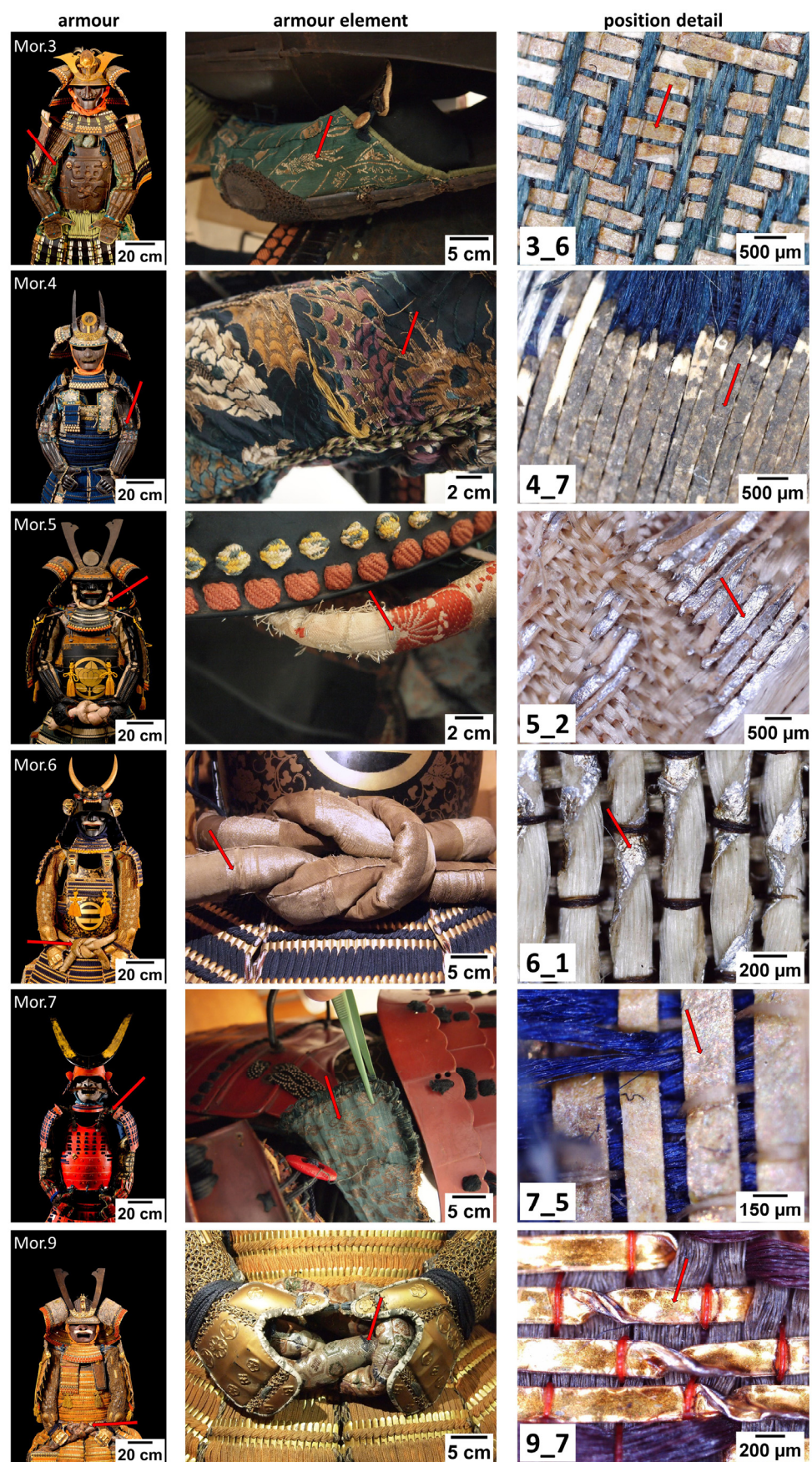


**Figure 1.** Images of the armors, the armor elements, and the position details.



### 2.5. Scanning Electron Microscopy and Energy Dispersive X-ray Spectroscopy

The samples were observed without any pre-treatment with a FEI/Philips XL30 ESEM (low vacuum mode—1 torr, 20 kV, BSE detector) (FEI Company, Hillsboro, OR, USA). The elemental analyses were carried out using an X-ray energy dispersive spectrometer, EDAX AMETEK Element (Ametek Inc., Mahwah, NJ, USA), coupled to SEM. Polished cross-sections were observed and analyzed, too.

The EDX detector is a silicon drift detector with a silicon nitride window. Depending on the situation, different acquisition modes were chosen, among area, point, line, and maps. Acquisition time was 30 s for point and area analyses, while acquisition was stopped manually for maps and lines when a good quality was obtained. A standardless eZAF method was used for a semiquantitative analysis of the samples.

The thickness of the metal layers and substrates of each sample was measured on the calibrated SEM images of polished cross-sections, using ImageJ software (Fiji version 1.53f51 [39]). For each layer, the thickness was measured at 5 random points, after which the mean and standard deviation of the measured values were calculated.

### 2.6. Infrared Spectroscopy

FTIR-ATR spectra were acquired by means of a Thermo Scientific Nicolet iS10 instrument (Thermo Fisher Scientific, Waltham, MA, USA), in the range between 4000 and 600  $\text{cm}^{-1}$ , 4  $\text{cm}^{-1}$  resolution, 32 scans. The background was periodically registered.

Spectra were interpreted by comparison with a homemade reference database and with the literature. Spectragryph optical spectroscopy software, Version 1.2.15, was used to visualize and manipulate FTIR-ATR spectra [40].

## 3. Results and Discussion

An overview of the characterization of each sample is presented in Table 2. Main results will be discussed below, starting with the *verso* (samples back side). Next, *recto* (samples front side) will be discussed. Finally, materials that were recognized as foreign to Japanese tradition will be treated separately.

**Table 2.** For each sample, results are presented together with a SEM image in BSE mode from the *recto* (scale bar: 50  $\mu\text{m}$  for sample 3\_6; 100  $\mu\text{m}$  for samples 4\_7, 5\_2, 6\_1, 7\_5, 9\_7).

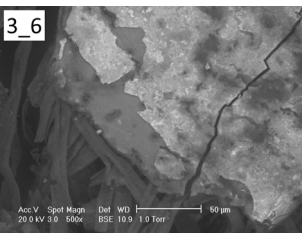
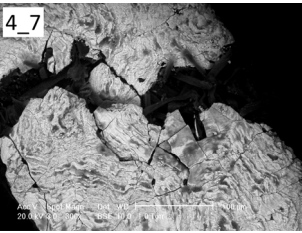
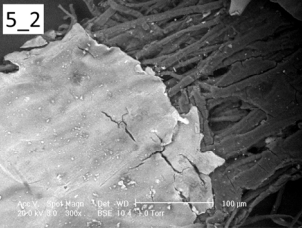
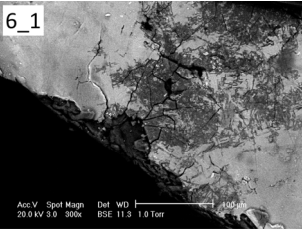
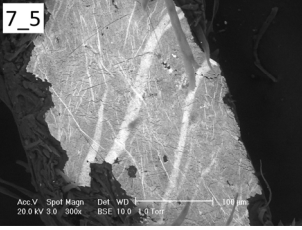
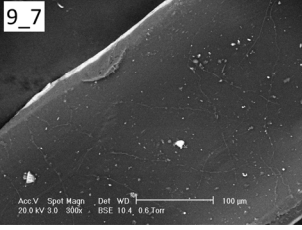
Sample	Metal Foil (Composition and Thickness)	Support Type and Thickness (With Associated Inorganic Compounds)	Inorganic Compounds Associated to <i>Recto</i> (Decay Materials, Fillers, etc. . . )	Organic Materials Associated to <i>Recto</i> (Adhesives, Covering Layer, etc. . . )
	Cu/Zn (92/8 weight %) $5.7 \pm 2.1 \mu\text{m}$	Paper (alunite, kaolinite) $85.7 \pm 3.9 \mu\text{m}$	Atacamite, paratacamite, alunite	Animal glue, rice starch
	Sn $2.3 \pm 0.4 \mu\text{m}$	Paper (alunite, gypsum, kaolinite) $80.2 \pm 12.8 \mu\text{m}$	Gypsum, kaolinite	Urushi

Table 2. Cont.

Sample	Metal Foil (Composition and Thickness)	Support Type and Thickness (With Associated Inorganic Compounds)	Inorganic Compounds Associated to <i>Recto</i> (Decay Materials, Fillers, etc. . . . )	Organic Materials Associated to <i>Recto</i> (Adhesives, Covering Layer, etc. . . . )
	Al upper layer $2.8 \pm 0.4 \mu\text{m}$ lower layer $2.7 \pm 0.2 \mu\text{m}$	Paper (alunite) upper layer $62.7 \pm 8.5 \mu\text{m}$	Syngenite, kaolinite	<i>Urushi</i>
	Al-Al/Mn Al/Mn layer $1.0 \pm 0.1 \mu\text{m}$ Al layer $3.8 \pm 1.0 \mu\text{m}$	Paper, wrapped around a rayon threads (alunite, syngenite) $17.4 \pm 9.1 \mu\text{m}$	Alunite, kaolinite	Animal glue
	Ag/Au (35/65 weight %) $1.1 \pm 0.2 \mu\text{m}$	Paper (alunite, bassanite, kaolinite) $57.6 \pm 7.0 \mu\text{m}$	Kaolinite, bassanite	<i>Urushi</i>
	Al $13.8 \pm 0.7 \mu\text{m}$	Cellophane $27.0 \pm 1.0 \mu\text{m}$		Natural rubber

The morphological analysis is fundamental to catch the complexity of layered structures and is the first step in the analysis of this type of sample. It can be seen, firstly, that samples are flat strips generally used for embroidery, except for sample 6\_1, which consists of a flat gilt strip wrapped around a thread.

Generally, samples back side shows a rich web of fibers arranged lengthwise. Fibrous support is visible on the *verso* or on the *recto* where metal foil is detached, and it appears generally pale-yellow colored (Figure 2). In addition, samples 3\_6, 4\_7, 6\_1, and 7\_5 show particulate matter on the *verso* (Figure 3a,b). Sample 5\_2 is different as it is the only strip showing a metal foil on both sides and, where metal foil is detached, fibers seem to be embedded in a gluey matter. 9\_7 is, on the contrary, made of metal only, with a transparent, homogeneous layer adherent on one side.



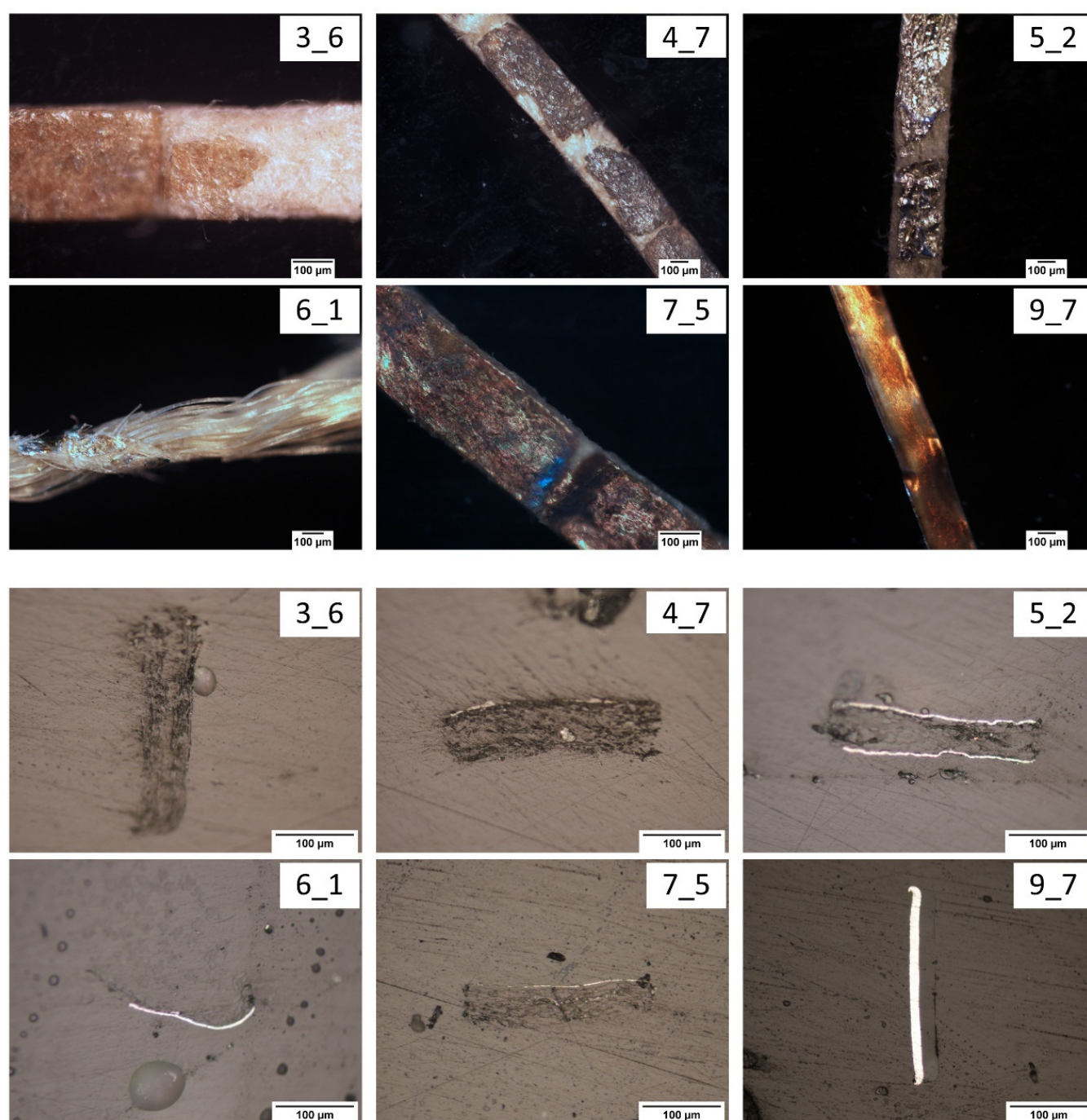


**Figure 2.** Optical microscopy images from samples *recto* (dark field modality—upper group) and cross-section (bright field modality—lower group) (scale bar: 100 µm).

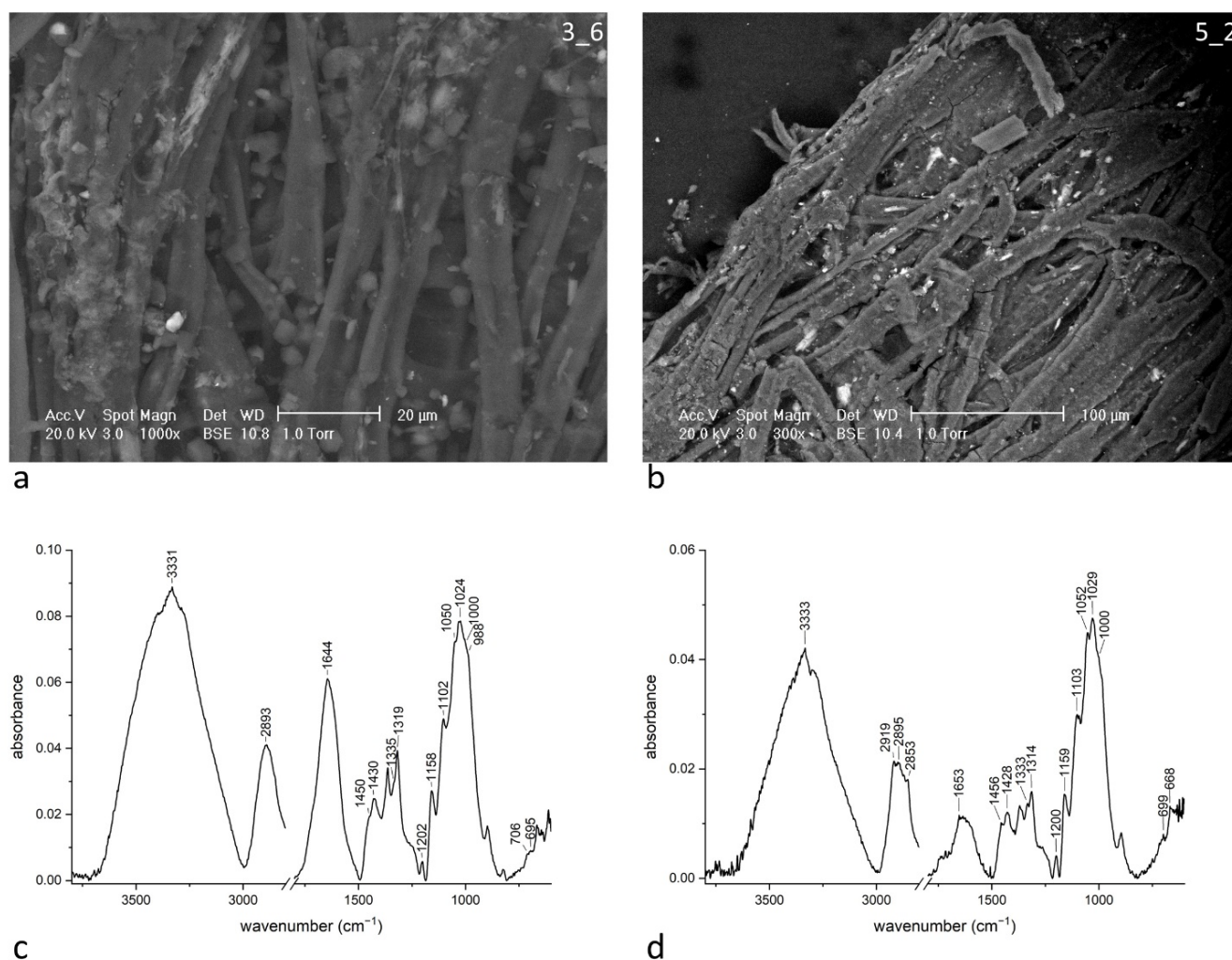


**Figure 3.** (a) SEM image in BSE mode of sample 3\_6 verso (scale bar: 20 μm); (b) SEM image in BSE mode of sample 5\_2 verso (scale bar: 100 μm); (c) ATR-FTIR spectrum of sample 3\_6 verso; (d) ATR-FTIR spectrum of sample 5\_2 verso. Spectra of samples 3\_6, 4\_7, 5\_2, 6\_1, 7\_5 verso are similar.

According to the historical information about *kinran* manufacture, the fibrous support is supposed to be made of *ko-zo* paper [15,18,19]. Thus, sample fibrous verso was analyzed through ATR-FTIR spectroscopy to get confirmation about the composition. In addition, sample verso was observed with SEM-EDX to obtain visual recognition of the paper and elemental information about the particulate matter.

The ATR-FTIR spectrum of sample 3\_6 verso is shown in Figure 3c as a representative of all spectra of this kind. The spectrum is dominated by the signals of a cellulose compound, in accord with the supposed material. The peak recognition is quite simple, due to high signal intensity. According to Marechal [41], in the region 950–1200 cm<sup>-1</sup> we easily recognize C-O stretching bands (1202, 1158, 1102, 1050, 1024, 1000, 988 cm<sup>-1</sup>). Bands at 705 and 665 cm<sup>-1</sup> and at 1450, 1430, 1335, 1315 cm<sup>-1</sup> are due to O-H bending in alcoholic groups. Finally, at high wavenumbers, we recognize C-H stretching band around 2900 cm<sup>-1</sup>. Signals which are attributable to O-H stretching modes in alcoholic groups, including the hydrogen bonds, are not distinguishable due to the water content, which makes it appear as broad bands around 3331 and 1644 cm<sup>-1</sup>.

Even though all the samples' verso consists of cellulose, small differences could be found. All spectra exhibit a broad peak at 2900 cm<sup>-1</sup>, except for sample 5\_2 (Figure 3d) and partially for sample 7\_5, which show also signals at 2919 and 2853 cm<sup>-1</sup>, and signals in the

zone 1800–1400  $\text{cm}^{-1}$ , which are consistent with the presence of *urushi*. It is not surprising, as both samples 5\_2 and 7\_5 are part of the *urushi* group (see below for peak discussion).

SEM images were taken from all fibrous samples and morphology is coherent with the attribution to paper [42]. In particular, samples 6\_1 and 7\_5 show that at least a part of the fibers is characterized by dislocations, which are attributable to a bast fiber (such as flax and hemp) [42].

EDX analysis was performed on areas or on some points to get a representative information from the sample surface. In spectra, most of the signal comes from carbon and oxygen content. In Table 3, elements that appear more abundantly are reported. Semi-quantitative analysis permitted to discriminate major elements against trace elements. Sample 5\_2 is covered with a metal foil on both sides, so elemental information comes from fibrous core as it appears from the cross-section. Sample 9\_7 is not discussed as it does not show a fibrous support.

**Table 3.** A list of the samples with an indication of elemental abundance of foreign elements.

Sample	Major Elements	Trace Elements
3_6	Al	Si, S, Ca, K
4_7	S, Ca	Al, Si, K
5_2	Na, Cl	Al, S, K
6_1	S, Ca, K	Al, Cl
7_5	S, Ca	Al, Si, K, Na, Cl

Calcium and sulphur appear frequently among fibers (samples 4\_7, 6\_1, 7\_5), suggesting the presence of gypsum ( $\text{CaSO}_4 \cdot 2\text{H}_2\text{O}$ ). When also potassium appears with a similar intensity, as for sample 6\_1, syngenite ( $\text{K}_2\text{Ca}(\text{SO}_4)_2 \cdot \text{H}_2\text{O}$ ) is supposed to be present. FTIR spectroscopy partially supports the interpretation, as the peculiar peaks at 1192, 1139, 1124, 1108, 1103  $\text{cm}^{-1}$  could be recognized. As for gypsum, the peaks at 3535, 3400, 1620, 670  $\text{cm}^{-1}$  in the spectrum of sample 4\_7 are confirmatory [43]. For sample 7\_5, bassanite ( $\text{CaSO}_4 \cdot 0.5(\text{H}_2\text{O})$ ), is proposed instead of gypsum on the base of peaks at 3610, 3408, 1153, 1116, 1096  $\text{cm}^{-1}$ .

Besides sulphur, all samples show aluminum and potassium signals of medium intensity. According to references [44,45], Japanese *ko-zo* paper for prints was seldom treated with clay or calcium carbonate to obtain a smoother surface, and even with a solution of potassium alum ( $\text{KAl}(\text{SO}_4)_2 \cdot 12\text{H}_2\text{O}$ ) and animal glue to give additional body and strength to the paper. Actually, alum is an important ingredient for papermaking also in Western tradition. As a consequence, we propose that the ubiquitous presence of aluminum, sulphur, and potassium is related to the use of alum also in Japanese papermaking processes. FTIR spectroscopy partially confirms the hypothesis, as peaks at 1225, 1159, 1083, 1024  $\text{cm}^{-1}$  should refer [46] to alunite ( $\text{KAl}_3(\text{SO}_4)_2(\text{OH})_6$ ), a common source of alum in the pre-industrial era.

Silicon content, which appears in samples 3\_6, 4\_7, and 7\_5, is probably related to small amounts of clay, together with a part of aluminum signal [47].

Figure 2 shows the *recto* and polished cross-section images of samples taken by optical microscopy. The metal foil covered layer appears very differently among samples. Two out of six are silver-colored, the other gold-colored (Table 1). Samples 3\_6 and 4\_7 do not show a metallic luster. Sample 5\_2 seems to be metal without any cover layer, while the others show a yellowish cover layer. Actually, images from the cross-section have been taken in bright field modality, which highlights the presence of metallic layers, which appear white-scale. In particular, sample 9\_7 is covered on one side only with a thick homogeneous layer, which could be responsible for the gold-like color. Cross-section analysis highlights also the strip thickness (Table 2) and allows us to appreciate the precision which was paid during manufacturing. In particular, samples 4\_7 and 7\_5 show great uniformity in thickness, which is probably related to great care taken during manufacturing. It is interesting to note that they are both among the most ancient armors.



ATR-FTIR spectra of the *recto* (Figure 4) show more variability respect to *verso*. Generally speaking, spectra have low intensities, which make interpretations more difficult. All spectra exhibit a doublet at 2922 and 2853  $\text{cm}^{-1}$  and an intense peak at 1632  $\text{cm}^{-1}$ . A shoulder appears at 1550  $\text{cm}^{-1}$ , but is more defined in sample 3\_6 and 6\_1 (Figure 4a), while the others show a broader peak with a specific fine structure together with a more visible shoulder at 1715  $\text{cm}^{-1}$  (Figure 4b). The region between 1500 and 1200  $\text{cm}^{-1}$  is quite similar among all samples. The broad band between 1200–1000  $\text{cm}^{-1}$  probably reflects the signal of cellulose. Some small peaks add up to broad cellulose bands, which will be discussed later. For example, sample 4\_7 exhibits a doublet at 1190–1134  $\text{cm}^{-1}$  and two shoulders at 3535 and 3400  $\text{cm}^{-1}$ . Under 1000  $\text{cm}^{-1}$ , the peaks do not show differences, except for a peak at 825  $\text{cm}^{-1}$ , which is specific to sample 3\_6. The same sample also exhibits a shoulder at 3440  $\text{cm}^{-1}$ .

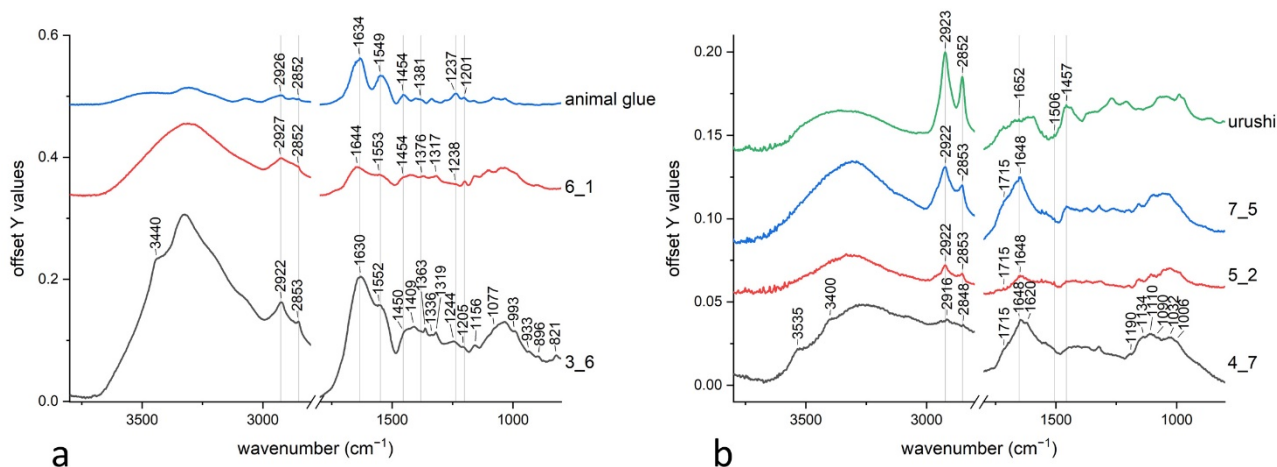


**Figure 4.** (a) ATR-FTIR spectra of samples 3\_6 and 6\_1 *recto*, and of a reference of animal glue (b) ATR-FTIR spectra of samples 4\_7, 5\_2, 7\_5 *recto*, and of a reference of urushi.

EDX results have been fundamental to get elemental information about inorganic parts of threads, most of all the metal foil. Punctual analysis permitted to obtain spectra for semi-quantitative analysis, such as for alloys ratio. Elemental maps and line spectra have been chosen to get spatial information together with an elemental one. Actually, the EDX technique is subject to error with a multi-layered sample, as secondary electrons come from more than one layer. To overcome the problem, cross-sections have been prepared and analyzed since this technique permits to obtain important information about metallic layers, even in presence of very complex stratigraphies [48]. Moreover, they offered the interesting possibility to perform profile analysis, as line spectra mode permitted to follow changes in elemental abundance from the surface to the core of sample.

Table 4 reports the composition of metal foils and the presence of foreign elements, which could be associated to degradation products or layers beneath the metal foil.

**Table 4.** A list of the samples under analysis with an indication of elemental abundance from *recto*.

Sample	Foil Composition	Major Elements	Trace Elements
3_6	Cu-Zn (alloy)	Cl	S, K, Al
4_7	Sn	Al	S, Ca, Si
5_2	Al	S, Ca, K, Al, Si	Cl
6_1	Al/Mn		Cl, S, K, Si
7_5	Au-Ag (alloy)	S, Ca, Al	K, Si
9_7	Al		Cl

The stratigraphy of each sample is summarized in Table 2, while the most interesting results are extensively described and discussed in the following sections. It appears clearly



that the metal constitutes the foil, or the metals if alloys are present. Where it was useful, maps and line spectra performed on cross-section are shown, accompanying a precise description of a part of the stratigraphy. For the sake of clarity, samples have been grouped and discussed according to the nature of the main organic compound revealed by analyses. An *urushi* group, an animal glue group and a group of samples emerging from other categorization (non-traditional materials group) were identified.

### 3.1. Urushi Group

References [15,18,19] report that *urushi* was the main choice as adhesive to join together paper and metal foil. In our study it was recognized in three samples, which are 4\_7, 5\_2, and 7\_5 (Figure 4b).

The main constituents of *urushi* are catecols with long chain substitution at the meta position. They also generally present one to three unsaturations in the side-chain, which are responsible for the auto-polymerization capability of the lacquer [49]. A home-made reference of *urushi* was compared with the samples, but also the study by Xia [49] was taken into account, as *urushi* spectrum is subjected to great changes during ageing. While the peak at around  $1730\text{ cm}^{-1}$  (C=O stretching) increases due to the formation of oxidation product, the peak at  $990\text{ cm}^{-1}$  (C-H out-of-plane bending) disappears as conjugate triene totally reacts in the auto-polymerization process. Also peaks at  $1620$  and  $1595\text{ cm}^{-1}$  (ring C=C stretching) disappear, due to changes of the vibration of double bonds because of the formation of dimers or polymers.

The peaks at  $2925$  and  $2850\text{ cm}^{-1}$  are strong and attributable to  $\text{CH}_2$  stretching of side chain. The bands around  $1650\text{ cm}^{-1}$  are due to C-C stretching, while the peak at  $1457\text{ cm}^{-1}$  is due to  $\text{CH}_2$  bending. The pattern of weak peaks between  $1600$  and  $1500\text{ cm}^{-1}$  is typical of *urushi* too, even if a complete assignation for these signals has never been proposed, except for the peak at  $1506\text{ cm}^{-1}$  which is attributable to a combination band of catechol (C-C + C-H stretching).

In samples 4\_7 and 5\_2, *urushi* was used as adhesive and probably as a covering layer on the metallic surface, as shown by SEM images (Figure 5). The morphology appears quite different, even if both share a non-bare metal surface.

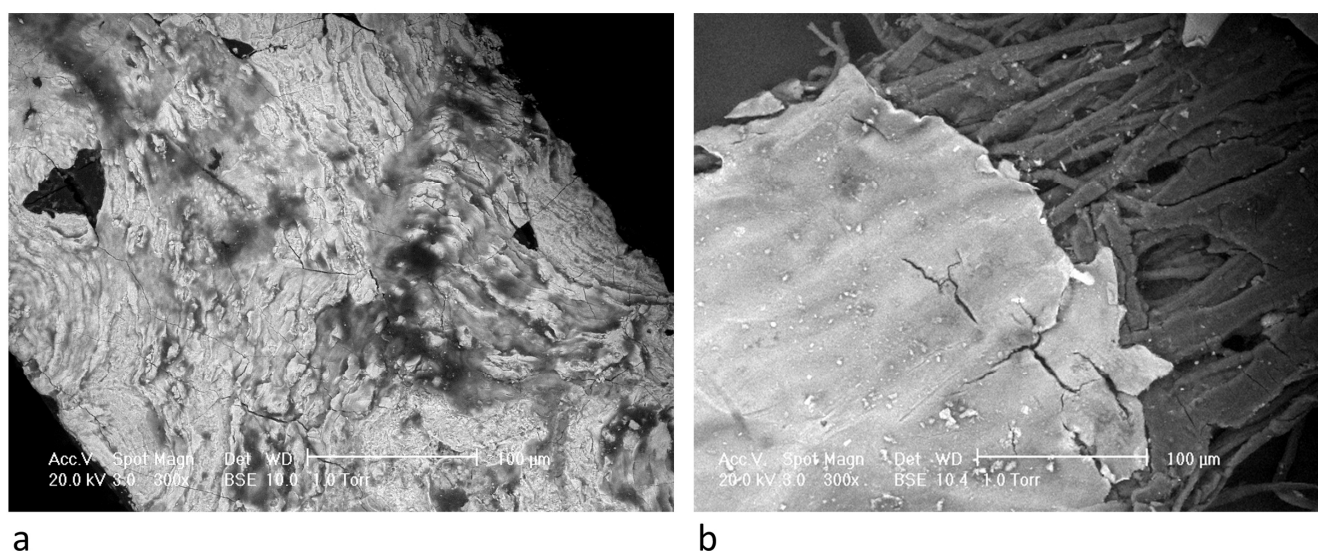


**Figure 5.** (a) SEM image in BSE mode of sample 4\_7 recto (scale bar: 100 µm) (b) SEM image in BSE mode of sample 5\_2 recto (scale bar: 100 µm).

Sample 4\_7 (Figure 5a) is characterized by a tin foil, with traces of copper. The cross-section does not show any discontinuity within the tin layer; on the contrary, the same layer appears corrugated, and its thickness varies a lot. EDX analysis performed on the surface shows the presence of sulphur and calcium, together with silicon and aluminum. FTIR

spectrum reports the presence of gypsum ( $3535, 3400, 1620, 1190, 1134, 1110, 670\text{ cm}^{-1}$ ) [46] and is compatible with the presence of kaolinite ( $\text{Al}_2(\text{OH})_4\text{Si}_2\text{O}_5$ , peaks at  $1115, 1090, 1032, 1006\text{ cm}^{-1}$ ) [46], which is indicative of the use of a clay [50]. To sum up, our hypothesis is that *urushi* was mixed with gypsum and clay powder to obtain a paste that was spread on an intentionally corrugated tin layer. The pursued effect was maybe the so called *sabi-nuri*, which was diffused as a finishing effect for armor metal plates to give the appearance of russet iron [23].

Sample 5\_2 (Figure 5b) is covered on both sides by an aluminum foil. EDX analysis shows that the superficial layers are rich of sulphur, calcium, potassium, silicon, and aluminum. As a small amount of particles appears on the surface, it is evident that inorganic compounds are located under the metal foil, probably mixed with *urushi* to work as a ground layer, which was common in lacquerware manufacturing [51,52] and also in Western gilding techniques with different binders [53]. FTIR analysis shows that the compounds are probably syngenite ( $\text{K}_2\text{Ca}(\text{SO}_4)_2 \cdot \text{H}_2\text{O}$ ) and kaolinite ( $\text{Al}_2(\text{OH})_4\text{Si}_2\text{O}_5$ ), as previously discussed.

Also, sample 7\_5 shows spectral features of *urushi* (Figure 4b). Elemental analysis shows that the fibrous core is covered with a metal foil constituted of silver and gold (Ag/Au ratio is 35/65 weight %). The cross-section analysis (Figure 6) does not show the presence of layers in the metal foil, so we can exclude the possibility of a gold gilding of a silver support [26]. In particular, the line analysis (Figure 6b) shows that sulphur content is mainly associated with the outer layer of silver and gold alloy, and slightly comes from inner layers as sulphate salts, as commonly found in some other samples. As a consequence, it is evident that it is chemically associated to silver ( $\text{Ag}_2\text{S}$ ), giving the well-known phenomenon of silver darkening [54]. EDX analysis of the surface evidences the presence of sulphur, calcium, aluminum, and, in lesser quantity, of potassium and silicon. According to FTIR spectrum, it is suggested there was the use of a small quantity of bassanite and kaolinite as ground layer.

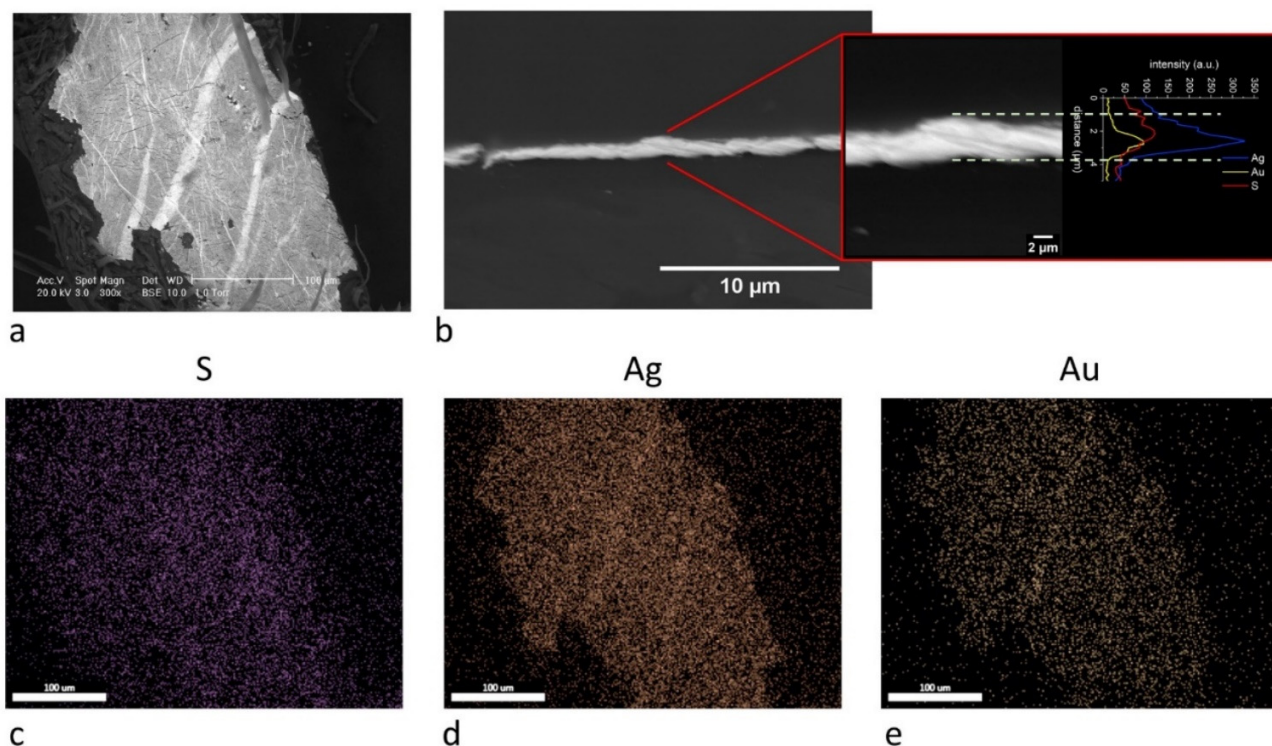


**Figure 6.** (a) SEM image in BSE mode of sample 7\_5 *recto* (scale bar: 100 µm), (b) elemental EDX line spectrum (scale bar: 10 and 2 µm) on polished cross-section and elemental distribution maps (scale bar: 100 µm) of (c) sulphur, (d) silver, and (e) gold on the surface of the sample.

### 3.2. Animal Glue Group

The peaks at 2922, 2853, 1633, 1550, 1451, 1377, 1317, 1237, 1201  $\text{cm}^{-1}$  are present in spectra from samples 3\_6 and 6\_1 *recto* (Figure 4a) and are attributable to animal glue. According to Derrick [55], the characteristic absorption bands are due to C-H stretching bands (2922, 2853  $\text{cm}^{-1}$ ), C=O stretching band (1633  $\text{cm}^{-1}$ ), C-N-H bending band (1550  $\text{cm}^{-1}$ ), C-H bending band (1451, 1377, 1317  $\text{cm}^{-1}$ ). Such a result is not surprising, as the use of deer glue (*nikawa*) is reported in the manufacture of *ukiyo-e* prints [44], colored photographs [56], armors [23], and lacquered objects [52]. Sample 6\_1, which appears mostly silver colored, was originally golden as some traces suggest (Figure 1), so animal glue with its yellowish shade probably formed a covering layer too.

Besides that, it appears clearly that in sample 3\_6, animal glue is mixed with rice starch. According to Derrick [55], the band at 2922  $\text{cm}^{-1}$  is attributable to C-H stretching, the signal at 1638  $\text{cm}^{-1}$  to O-H bending, the peaks at 1452, 1416, 1335  $\text{cm}^{-1}$  to C-H bending, the peaks at 1245, 1206, 1150, 1077, 995, 930, 896  $\text{cm}^{-1}$  to C-O stretching. Also rice starch is known to be a Japanese traditional adhesive material (*funori*), especially for paper, and is reported to be mixed with *urushi* (*mugi urushi*) for armor lacquering [23].

Sample 3\_6 appears decayed (Figure 7a), as most of the metal foil is detached from the thread (Figure 1). The foil is an alloy of copper and zinc (Cu/Zn ratio is 92/8 weight %), which is more similar to orichalcum or pinchbeck than to brass. Orichalcum, which means “mountain copper”, was common among Greeks and Roman, who took it into great consideration and appreciated its golden red shade [57]. We can suppose that it was not considered a merely low-cost substitute for gold in Japan, too. Pinchbeck has a similar composition and appeared in Europe in the early 18th century by Christopher Pinchbeck, a London clock and watchmaker [58].

Elemental maps (Figure 7c–f) show also a spatial correlation of copper and chlorine. Some common decay products of brass are atacamite ( $\text{Cu}_2\text{Cl}(\text{OH})_3$ ) and paratacamite ( $(\text{Cu,Zn})_2(\text{OH})_3\text{Cl}$ ), and their spectral features appear with prominent peaks at 3440 and 820  $\text{cm}^{-1}$  [46]. Sulphur presence is apparently related to copper too. Actually, the line spectrum (Figure 7b) shows that copper and chlorine are effectively associated across the metal foil, showing a homogenous decay, which could be the cause of the extensive detachment of the foil. On the contrary, the increase of sulphur concentration is visible immediately 5  $\mu\text{m}$  under the metal foil, suggesting that alum (also potassium and aluminum signals appear) was mixed with animal glue and starch to obtain the adhesive for the metal foil. Such a compound is reported to be used in *ukiyo-e* manufacturing under the name of *doza* [44].

Sample 6\_1 apparently shows an aluminum-manganese alloy metal foil. Aluminum and manganese show the same spatial distribution (Figure 8c,d), and they clearly appear related to the metal foil. Cross-section analysis is particularly interesting, as a separation between two layers of metal foil appears clearly (Figure 8a,b). Aluminum constitutes the inner layer, while manganese is present in the thin, superficial layer as a component of the aluminum/manganese alloy. Mn concentration varies from 18% to 35% in the alloy. The former concentration ratio was obtained with an acceleration voltage of 20 kV, the latter of 15 kV. Reducing the acceleration voltage also the drop-shape volume, which detected X-rays come from, is reduced, so the measure is more accurate [26]. Aluminum-manganese alloys are reported to be protective against corrosion [59].



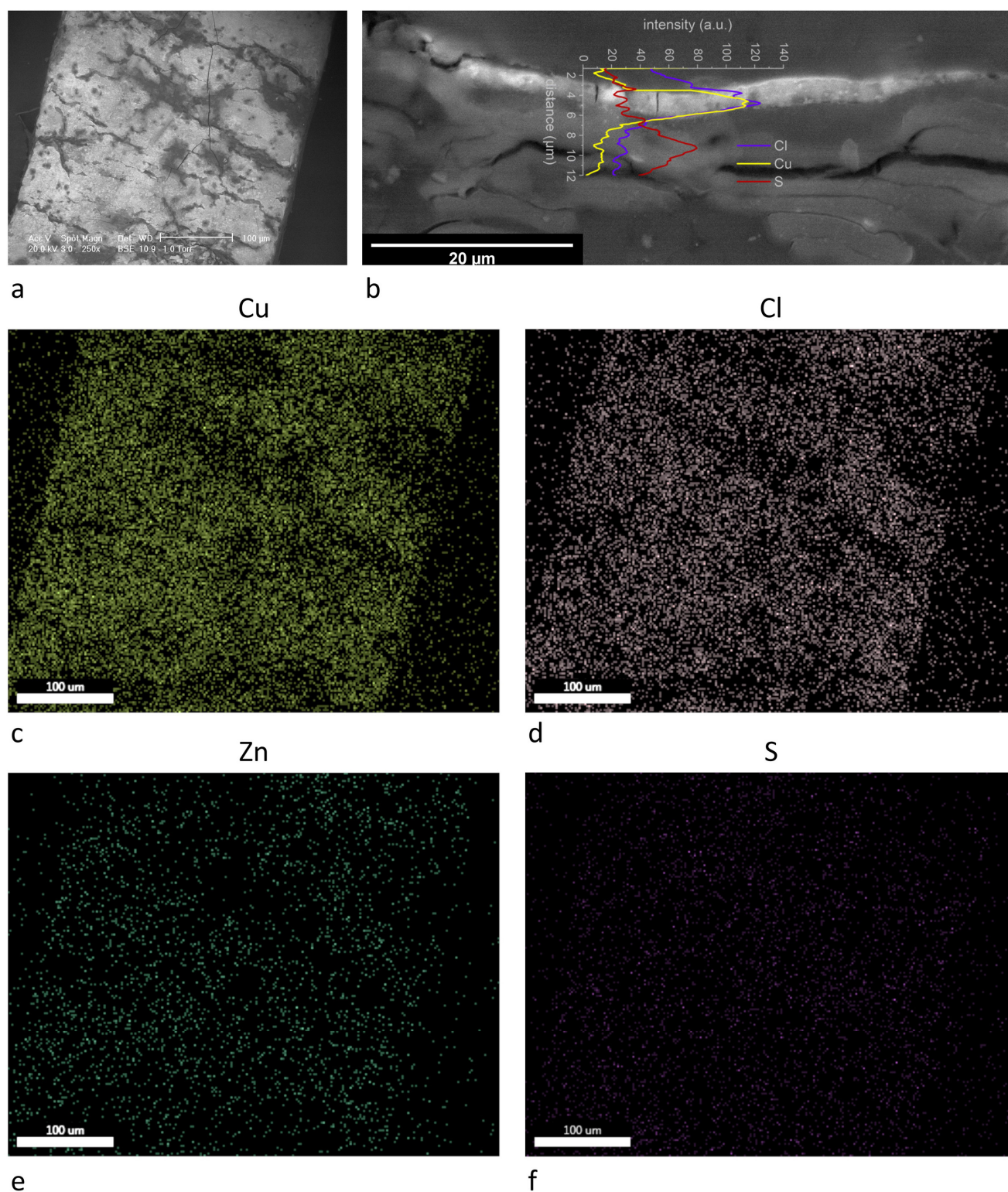


**Figure 7.** (a) SEM image in BSE mode of sample 3\_6 recto (scale bar: 100 µm), (b) elemental EDX line spectrum (scale bar: 20 µm) on polished cross-section and elemental distribution maps (scale bar: 100 µm), of (c) copper, (d) chlorine, (e) zinc, and (f) sulphur on the surface of the sample.



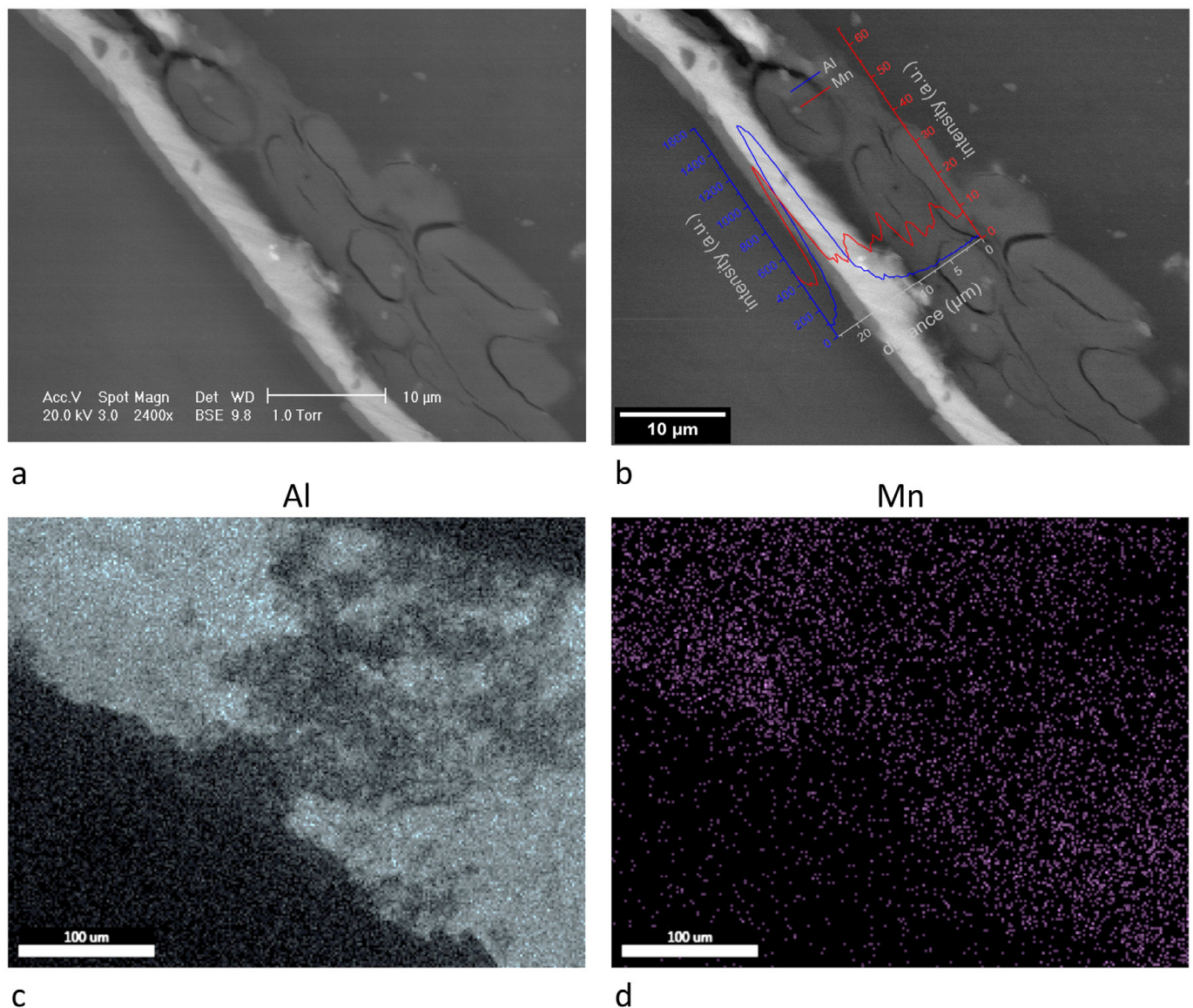


**Figure 8.** (a) SEM image in BSE mode of a detail of sample 6\_1 cross-section (scale bar: 10 µm), (b) elemental EDX line spectrum (scale bar: 10 µm) on polished cross-section and elemental distribution maps (scale bar: 100 µm) of (c) aluminum and (d) manganese on the surface of the sample.

The EDX analysis highlights the presence of sulphur, potassium, and silicon. Assuming that the aluminum signal does not come only from the metal foil, we can propose the presence of alunite ( $\text{KAl}_3(\text{SO}_4)_2(\text{OH})_6$ ) and kaolinite ( $\text{Al}_2(\text{OH})_4\text{Si}_2\text{O}_5$ ). FTIR spectroscopy partially confirms the hypothesis, as peaks at 1225, 1159, 1083, 1024  $\text{cm}^{-1}$  should refer to alunite [46], and at 1115, 1090, 1032, 1006  $\text{cm}^{-1}$  to kaolinite [46]. They are probably related to compounds mixed to the glue layer under metal foil.

### 3.3. Non-Traditional Materials

On the basis of the organic compounds detected on the threads, sample 9\_7 and the threads from sample 6\_1 core (Figure 9) form a separate group of materials which do not belong to Japanese tradition.

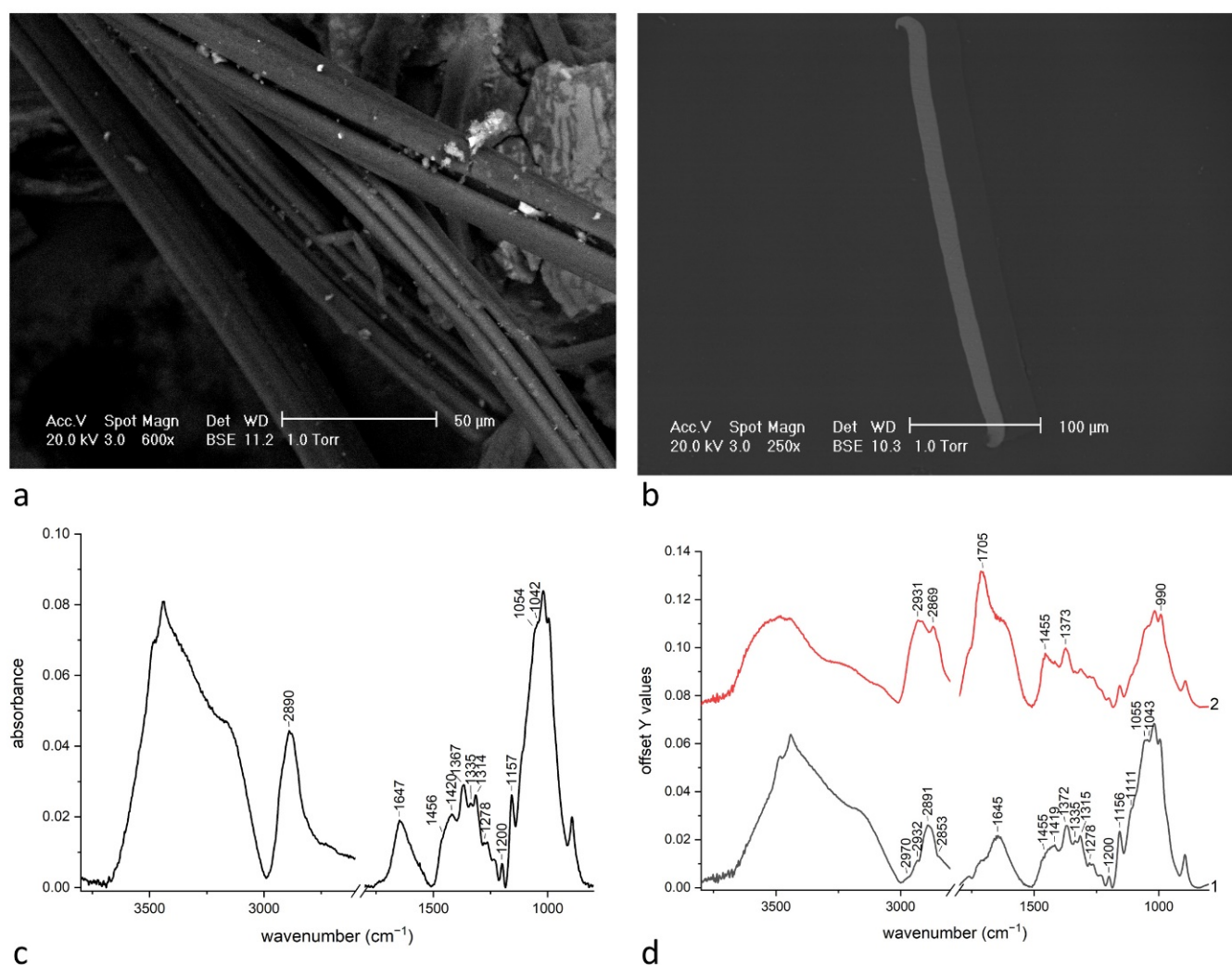


**Figure 9.** (a) SEM image in BSE mode of sample 6\_1 (scale bar: 50 μm), (b) SEM image in BSE mode of a cross-section of sample 9\_7 (scale bar: 100 μm), (c) ATR-FTIR spectrum of thread which constitutes the core of sample 6\_1, (d) ATR-FTIR spectra of sample 9\_7 recto, constituted by a transparent foil only (1) or by a transparent foil with traces of a yellow substance (2).

Sample 9\_7 immediately appears different from all the other samples as it is made of metal only, with a thick, homogeneous layer adherent on one side. Sample 6\_1 core is the most complex as it consists in a flat gilt strip wrapped around a thread formed by some fibers. On the basis of the morphological analysis, this thread appears to be made of artificial fibers due to the uniformity and typical longitudinal striations [60]. ATR-FTIR spectrum of the *recto* of sample 9\_7 (Figure 9d, 1) surprisingly strictly resembles that of the thread, which constitutes the core of sample 6\_1 (Figure 9c).

As for sample 9\_7, ATR-FTIR spectrum of *verso* is not shown due to the low intensity of signal, which allows us to think that no organic substances are present. The *recto* was analyzed as-is and after the mechanical removal of transparent foil, which was adherent to aluminum foil. Spectra from the *recto* and from the transparent foil with traces of yellow substance are shown (Figure 9d, 1 and 2), showing signal from the transparent foil. Actually, between the two spectra, some significant differences arise, which are located at CH<sub>2</sub> stretching range near 2900 cm<sup>-1</sup> and between 1800–1400 cm<sup>-1</sup>.

According to the literature [61], spectra from the transparent foil and from the core threads show the spectral features of regenerated cellulose. The band at 3000 cm<sup>-1</sup> is due to OH stretching from hydrogen bonds; peaks at 2970, 2932, 2890 cm<sup>-1</sup> to C-H stretching; peak at 2853 cm<sup>-1</sup> to CH<sub>2</sub> asymmetric stretching. The bands at 1645, 1455, 1335, 1200 cm<sup>-1</sup> are due to OH vibration modes; peaks at 1420, 1370, 1315, 1278 cm<sup>-1</sup> to C-H and C-H<sub>2</sub>

vibrations. Finally, peak at  $1155\text{ cm}^{-1}$  is due to C-O-C vibration, at  $1111\text{ cm}^{-1}$  to ring vibration, at  $1055$  and  $1042\text{ cm}^{-1}$  to C-O stretching. These peaks are peculiar for both cellophane or viscose [61], which are both made of regenerated cellulose.

As sample 6\_1 core thread is a fiber with artificial characteristics, there is no doubt that it is viscose, a cheaper substitute for silk, which was patented in 1902.

It is clear that also sample 9\_7 stands out from Japanese tradition. Aluminum foil, which is definitely thicker than traditional metal foil, shows in its cross-section a double hooked shape that is conceivable only with an industrial process. The transparent foil which is adherent to the metal can be effectively cellophane, as J    [14] found that some modern metallic threads were made by an aluminum strip coupled with a cellophane foil (such a product was commercialized since 1939 with the name of “Cellometal”). This material, or the adhesive that was used to join the two foils, is yellowish, modifying the natural color of aluminum with a golden shade. Gorassini et al. [62] found that some historical adhesive tapes were made of cellophane with an adhesive based on synthetic (styrene-isoprene copolymer) or natural rubber (cis-polyisoprene). He reports FTIR spectra of all materials he studied, including that of aged rubber. In particular, the peculiar peaks of the yellow substance, which are mainly at  $2931$ ,  $2870$ ,  $1705$ ,  $1455$ ,  $1373$ ,  $990\text{ cm}^{-1}$ , allow us to recognize the use of natural rubber (Figure 9b, spectrum 2). The assignments of main absorption peaks for aged natural rubber adhesive are observed at  $2924$  and  $2854\text{ cm}^{-1}$  assigned to  $\text{CH}_2$  and  $\text{CH}_3$  stretching, respectively. peaks at  $1449$  and  $1375\text{ cm}^{-1}$  are due to C-H deformation of  $\text{CH}_2$  and  $\text{CH}_3$  groups, respectively. The absorption at  $1663\text{ cm}^{-1}$ , which is assigned to C-C stretching for unaged rubber, is partially covered by the band at  $1700\text{ cm}^{-1}$  due to oxidation products. Peaks from styrenic compounds, typical of synthetic rubber, are absent.

#### 4. Conclusions

The analyses, conducted with well-tested techniques, returned solid results of particular importance, since Japanese metallic threads (*kinran*) have never been investigated before despite similar Western artefacts. The research offers new insights and data on the materials and techniques of Japanese applied art, even if based on a small nucleus of samples, and could stimulate new research to expand the references database of scholars of ancient armors.

Great variability was recognized in the samples, showing that the topic is more complex than expected and is worthy of in-depth studies. A first distinction can be made between traditional techniques, found in most samples, and industrial ones, recognized in modern threads, which started to appear along 20th century, as the presence of a “Cellometal” sample shows. This sample delays the dating of the armor Mor.9 by a few decades, as the material started to be produced in 1939. Actually, it is possible that only the sash must be post-dated, as it was a part of the equipment which was easily damaged and substituted. Yet, even the more recent samples surprisingly showed that traditional techniques were largely maintained. It was in fact proved that modern materials, as such aluminum, could coexist with traditional ones, such as *urushi*, and with the traditional technique of gluing a thin metal foil on a paper support. The materials used with this peculiar technique have been investigated, obtaining precious information both for the organic and the inorganic parts. Mediating on all samples that show a traditional manufacture, it can be said that the support was made of paper treated with alum salts. The adhesives were both animal glue and *urushi*, and rice starch appears as a coadjuvant in a case. Clay and gypsum minerals were mixed with the adhesive and spread under the foil, similarly to the use of “bolus” for gilding in the West [53], or on the surface probably to achieve special effects.

Particularly interesting is the evolution over the centuries in the use of metals. While throughout the 17th, 18th, and 19th centuries silver and gold alloy and orichalcum (copper-zinc alloy) were chosen to obtain gilt strips, since the Meiji period (1868–1912), aluminum was preferred, both for a gold and a silver color effect. It is probable that at least until 1886



(when the process Hall-Heroult for the economically profitable aluminum production was developed), this metal was not a cheap substitute for precious metals, but it was specifically chosen for its features, such as high malleability, reflectiveness, and corrosion resistance. For example, it visually resembles silver, both in color and in the great ability to reflect light, but it is not subjected to darkening. As our research demonstrated, aluminum was used as is when its naturally silver color was requested, even with a manganese alloy layer, which enhanced corrosion resistance. For a gold effect, metal foil was covered with a layer of naturally yellow substances, as the tradition suggested [23].

The study permitted also to clarify the context of armor production in relation with the period of its manufacturing (e.g., the social status of the owner, etc.). The choice of the metal by the craftsman reflects the wealth of the commissioner. Aluminum was surely a cheap substitute in the 20th century, as well as rayon. The use of industrial metallic thread as “Cellometal” is similarly a way to reduce costs. Actually, also during the pre-industrial period, gold and silver appeared much less diffused as previously thought. Since Marco Polo’s report told about the “Gold Island”, Japan was considered by the West to be very rich in gold mines, as he could see gilded shrines, but it should be noted that at that time gold was not used as currency. Actually, the country has historically been scarcely rich enough to satisfy the domestic demand, but silver was the real abundant feedstock [63,64]. Meanwhile, gold color was charged with religious and philosophical meanings, which explains its great diffusion and the search for techniques to imitate its appearance. Our study demonstrated that gold was only the minor part in silver-gold alloys and that orichalcum was used, too. Actually, there is also the possibility that the red golden shade, which is typical of this alloy, was a pursued effect [57].

The most surprising result is the use of the tin foil. Literature does not report the use of tin, which generally does not show particularly interesting aesthetic characteristics [65]. Besides that, the sample differs from others for roughness and for the presence of gypsum and clay on the surface mixed with *urushi*. Our hypothesis is that the pursued effect was maybe the so called *sabi-nuri*, which was diffused as a finishing effect for armor metal plates to give the appearance of russet iron [23].

With regard to the methodologies developed in this work, SEM images of the cross-sections have been presented with a line spectrum, in addition to traditional elemental maps. This way of reporting the results is in fact particularly informative for studying thin gilding on a bulk metal core. In general, it seems a very useful tool in case of unclear superficial maps, when also a cross-section is available. Compared to maps from the cross-section, line spectrum has the advantage of mathematical visualization of intensities vs. distance and the possibility to have a quantification as with point analysis.

**Author Contributions:** Conceptualization, M.L. and L.R.; Investigation, C.C., L.G., S.M., and L.R.; Writing—original draft preparation, C.C., L.G., M.L., and L.R.; Writing—review and editing, F.P.C., C.C., L.G., M.L., S.M., L.R., and S.R. All authors have read and agreed to the published version of the manuscript.

**Funding:** This research received no specific grant from any funding agency in the public, commercial, or not-for-profit sectors.

**Institutional Review Board Statement:** Not Applicable.

**Informed Consent Statement:** Not Applicable.

**Data Availability Statement:** The data presented in this study are available on request from the corresponding author.

**Conflicts of Interest:** The authors declare no conflict of interest.



## References

- Járó, M. Gold embroidery and fabrics in Europe: XI–XIV centuries. *Gold Bull.* **1990**, *23*, 40–57. [\[CrossRef\]](#)
- Karatzani, A. Metal threads: The historical development. In *Proceedings of the Traditional Textile Craft: An Intangible Cultural Heritage?* Ebert, C., Frisch, S., Harlow, M., Strand, E.A., Bjerregaard, L., Eds.; University of Copenhagen: Copenhagen, Denmark, 2014; pp. 163–174.
- Csiszár, G.; Ungár, T.; Járó, M. Correlation between the sub-structure parameters and the manufacturing technologies of metal threads in historical textiles using X-ray line profile analysis. *Appl. Phys. A Mater. Sci. Process.* **2013**, *111*, 897–906. [\[CrossRef\]](#)
- Martínez, B.; Piquero-Cilla, J.; Montoya, N.; Doménech-Carbó, M.T.; Doménech-Carbó, A. Electrochemical analysis of gold embroidery threads from archaeological textiles. *J. Solid State Electrochem.* **2018**, *22*, 2205–2215. [\[CrossRef\]](#)
- Abdel-Kareem, O.; Harith, M.A. Evaluating the use of laser radiation in cleaning of copper embroidery threads on archaeological Egyptian textiles. *Appl. Surf. Sci.* **2008**, *254*, 5854–5860. [\[CrossRef\]](#)
- Hacke, A.M.; Carr, C.M.; Brown, A.; Howell, D. Investigation into the nature of metal threads in a Renaissance tapestry and the cleaning of tarnished silver by UV/Ozone (UVO) treatment. *J. Mater. Sci.* **2003**, *38*, 3307–3314. [\[CrossRef\]](#)
- Weiszburg, T.G.; Gherdán, K.; Ratter, K.; Zajzon, N.; Bendo, Z.; Radnóczy, G.; Takács, Á.; Vácz, T.; Varga, G.; Szakmány, G. Medieval Gilding Technology of Historical Metal Threads Revealed by Electron Optical and Micro-Raman Spectroscopic Study of Focused Ion Beam-Milled Cross Sections. *Anal. Chem.* **2017**, *89*, 10753–10760. [\[CrossRef\]](#) [\[PubMed\]](#)
- Ferreira, T.; Moreiras, H.; Manhita, A.; Tomaz, P.; Mirão, J.; Dias, C.B.; Caldeira, A.T. The Liturgical Cope of D. Teotónio of Braganza: Material Characterization of a 16th Century Pluviale. *Microsc. Microanal.* **2015**, *21*, 2–14. [\[CrossRef\]](#) [\[PubMed\]](#)
- Karatzani, A. Study and analytical investigation of metal threads from Byzantine/Greek ecclesiastical textiles. *X-ray Spectrom.* **2008**, *37*, 410–417. [\[CrossRef\]](#)
- Šimić, K.; Zamboni, I.; Fazinić, S.; Mudronja, D.; Sović, L.; Gouasmia, S.; Soljačić, I. Comparative analysis of textile metal threads from liturgical vestments and folk costumes in Croatia. *Nucl. Instrum. Methods Phys. Res. Sect. B Beam Interact. Mater. Atoms* **2018**, *417*, 115–120. [\[CrossRef\]](#)
- Duran, A.; Perez-Maqueda, R.; Perez-Rodriguez, J.L. Degradation processes of historic metal threads used in some Spanish and Portuguese ornamentation pieces. *J. Cult. Herit.* **2019**, *36*, 135–142. [\[CrossRef\]](#)
- Oraltay, R.G.; Karadag, R. Surface Investigation of Metal Threads and Solid Metals of Ottoman Textiles in the Topkapi Palace Museum. *Stud. Conserv.* **2020**, *65*, 59–64. [\[CrossRef\]](#)
- Muros, V.; Wärmländer, S.K.T.S.; Scott, D.A.; Theile, J.M. Characterization of 17th–19th century metal threads from the colonial Andes. *J. Am. Inst. Conserv.* **2007**, *46*, 229–244. [\[CrossRef\]](#)
- Járó, M.; Gál, T.; Tóth, A. The Characterization and Deterioration of Modern Metallic Threads. *Stud. Conserv.* **2000**, *45*, 95–105. [\[CrossRef\]](#)
- Gunsalus, H.C. *An Exhibition of Japanese Textiles*; The Art Institute of Chicago: Chicago, IL, USA, 1934; Volume 28.
- Moriyama, A. Japanese Textile Culture The Example of Junichi Arai and Five Other Creators. In *A Companion to Textile Culture*; Harris, J., Ed.; John Wiley & Sons: Hoboken, NJ, USA, 2020; pp. 353–370.
- Priest, A.; Simmons, P. *Chinese Textiles: An Introduction to Their History, Sources, Techniques, Symbolism, and Use*; The Metropolitan Museum of Art: New York, NY, USA, 1934.
- Nomura, S. *Ancient Chinese and Japanese Nishiki and Kinran Brocades*; N. Sawyer & Son: Boston, MA, USA, 1914.
- Neighbourgh Parent, M.; Japanese Architecture and Art Net Users System (JAANUS). Kinran. Available online: <http://www.aisf.or.jp/~{jaanus/> (accessed on 9 July 2021).
- Scidmore, E.R. Japanese textiles: Brocades and crapes. *Harpers Bazar* **1897**, *30*, 703.
- Parry-Williams, T. Made-by-hand: [Re]valuing traditional (Japanese) textile practices for contemporary design. *Craft Res.* **2015**, *6*, 165–186. [\[CrossRef\]](#)
- Robinson, H.R. *Oriental Armour*; Walker & Co.: New York, NY, USA, 1967.
- Sakakibara, K. *The Manufacture of Armour and Helmets in Sixteenth Century Japan (Cho-Kokatchu-Seisakuben)*; Robinson, H.R., Ed.; Charles E. Tuttle Company Inc.: Rutland, VT, USA; Tokyo, Japan, 1964.
- Perez-Rodriguez, J.L.; Perez-Maqueda, R.; Franquelo, M.L.; Duran, A. Study of the thermal decomposition of historical metal threads. *J. Therm. Anal. Calorim.* **2018**, *134*, 15–22. [\[CrossRef\]](#)
- Popowich, A.K.; Cleland, T.P.; Solazzo, C. Characterization of membrane metal threads by proteomics and analysis of a 14th c. thread from an Italian textile. *J. Cult. Herit.* **2018**, *33*, 10–17. [\[CrossRef\]](#)
- Nord, A.G.; Tronner, K. A Note on the Analysis of Gilded Metal Embroidery Threads. *Stud. Conserv.* **2000**, *45*, 274–279.
- Perez-Rodriguez, J.L.; Albardonedo, A.; Robador, M.D.; Duran, A. Spanish and Portuguese gilding threads: Characterization using microscopic techniques. *Microsc. Microanal.* **2018**, *24*, 574–590. [\[CrossRef\]](#)
- Bergstrand, M.; Hedhammar, E. European Metal Threads in Swedish Churches 1600–1751. *Stud. Conserv.* **2006**, *51*, 11–28. [\[CrossRef\]](#)
- Hacke, A.-M.; Carr, C.M.; Brown, A. Characterisation of metal threads in Renaissance tapestries. In *Proceedings of the International Conference on Metals Conservation*, Canberra, Australia, 4–8 October 2004; pp. 71–78.
- Karatzani, A.; Rehren, T. The use of metal threads and decorations in Byzantine-Greek Orthodox ecclesiastical textiles. *JOM* **2006**, *58*, 34–37. [\[CrossRef\]](#)
- Kohara, N.; Sasa, Y.; Sakurai, K.; Uda, M. A Note on the Characterization of Metal Threads in Historic Textiles Handed down by the Ainu People. *Stud. Conserv.* **1998**, *43*, 109–113.

32. Costa, V.; de Reyer, D.; Betbeder, M. A note on the analysis of metal threads. *Stud. Conserv.* **2012**, *57*, 112–115. [CrossRef]
33. Rezić, I.; Ćurković, L.; Ujević, M. Simple methods for characterization of metals in historical textile threads. *Talanta* **2010**, *82*, 237–244. [CrossRef]
34. Cybulska, M.; Jedraszek-Bomba, A.; Kuberski, S.; Wrzosek, H. Methods of chemical and physicochemical analysis in the identification of archaeological and historical textiles. *Fibres Text. East. Eur.* **2008**, *16*, 67–73.
35. Joosten, I.; Van Bommel, M.R.; Keijzer, R.H.D.; Reschreiter, H. Micro analysis on hallstatt textiles: Colour and condition. *Microchim. Acta* **2006**, *155*, 169–174. [CrossRef]
36. Ok, S.Y.; Seon, Y.L. Study on the Form and Character of Gold Thread in Weave with Supplementary Gold Wefts Embroidery. *J. Korean Soc. Costume* **2013**, *63*, 79–93.
37. Kim, J.E.; Yu, A.J.; Han, Y.B.; Chung, Y.J. Study of Characteristics for Red Adhesive in Traditional Gold Thread. *J. Korean Conserv. Sci.* **2016**, *32*, 43–49. [CrossRef]
38. Luraschi, M. *Il Samurai. Da Guerriero a Icona*; Silvana Editoriale: Milano, Italy, 2018.
39. Schindelin, J.; Arganda-Carreras, I.; Frise, E.; Kaynig, V.; Longair, M.; Pietzsch, T.; Preibisch, S.; Rueden, C.; Saalfeld, S.; Schmid, B.; et al. Fiji: An open-source platform for biological-image analysis. *Nat. Methods* **2012**, *9*, 676–682. [CrossRef] [PubMed]
40. Menges, F. Spectragryph—Optical Spectroscopy Software, Version 1.2.15 2021. Available online: <https://www.effemm2.de/spectragryph/> (accessed on 9 July 2021).
41. Maréchal, Y.; Chanzy, H. The hydrogen bond network in I( $\beta$ ) cellulose as observed by infrared spectrometry. *J. Mol. Struct.* **2000**, *523*, 183–196. [CrossRef]
42. Quagliarini, C. *Chimica Delle Fibre Tessili*; Zanichelli: Bologna, Italy, 1989.
43. Ranalli, G.; Bosch-Roig, P.; Crudele, S.; Rampazzi, L.; Corti, C.; Zanardini, E. Dry biocleaning of artwork: An innovative methodology for Cultural Heritage recovery? *Microb. Cell* **2021**, *8*, 91–105. [CrossRef]
44. Sasaki, S. Materials and Techniques. In *The Hotei Encyclopedia of Japanese Woodblock Prints*; Hotei Publishing: Amsterdam, The Netherlands, 2005; pp. 325–347.
45. Quattrini, M.V.; Ioele, M.; Sodo, A.; Priori, G.F.; Radechia, D. A seventeenth century Japanese painting: Scientific identification of materials and techniques. *Stud. Conserv.* **2014**, *59*, 328–340. [CrossRef]
46. Chukanov, N.V. *Infrared Spectra of Mineral Species—Extended Library*; Springer Science+Business Media: Dordrecht, The Netherlands, 2014; Volume 1, ISBN 9789400771277.
47. Bugini, R.; Corti, C.; Folli, L.; Rampazzi, L. Unveiling the Use of Creta in Roman Plasters: Analysis of Clay Wall Paintings From Brixia (Italy). *Archaeometry* **2017**, *59*, 84–95. [CrossRef]
48. Sansonetti, A.; Andreotti, A.; Bertasa, M.; Bonaduce, I.; Corti, C.; Facchin, L.; La Nasa, J.; Spiriti, A.; Rampazzi, L. Territory and related artworks: Stuccoworks from the lombard lakes. *J. Cult. Herit.* **2020**, *46*, 382–398. [CrossRef]
49. Xia, J.; Lin, J.; Xu, Y.; Chen, Q. On the UV-induced polymeric behavior of chinese lacquer. *ACS Appl. Mater. Interfaces* **2011**, *3*, 482–489. [CrossRef] [PubMed]
50. Bugini, R.; Corti, C.; Folli, L.; Rampazzi, L. Roman Wall Paintings: Characterisation of Plaster Coats Made of Clay Mud. *Heritage* **2021**, *4*, 48. [CrossRef]
51. Burmester, A. The scientific investigation of two Japanese dance masks. In Proceedings of the 17th International Symposium on the Conservation and Restoration of Cultural Property: Conservation of Urushi Objects, Tokyo, Japan, 10–12 November 1993; pp. 127–146.
52. Salvemini, F.; Grazzi, F.; Agostino, A.; Iannaccone, R.; Civita, F.; Hartmann, S.; Lehmann, E.; Zoppi, M. Non-invasive characterization through X-ray fluorescence and neutron radiography of an ancient Japanese lacquer. *Archaeol. Anthropol. Sci.* **2013**, *5*, 197–204. [CrossRef]
53. Giumlia-Mair, A.; Meriani, S.; Lucchini, E. Indagini archeometallurgiche su dorature antiche: Analisi, tecniche e varianti. In Proceedings of the I Bronzi Antichi: Produzione e Tecnologia, Grado-Aquileia, Italy, 22–26 May 2001; pp. 338–343.
54. Nord, A.G.; Tronner, K.; Thorén, C. Discolouration of Gold Decorations. *Stud. Conserv.* **2018**, *63*, 189–193. [CrossRef]
55. Derrick, M.; Stulik, D.; Laundry, J. *Infrared Spectroscopy in Conservation Science*; The Getty Conservation Institute: Los Angeles, CA, USA, 1999; ISBN 9781119130536.
56. Rampazzi, L.; Brunello, V.; Campione, F.P.; Corti, C.; Geminiani, L.; Recchia, S.; Luraschi, M. Non-invasive identification of pigments in Japanese coloured photographs. *Microchem. J.* **2020**, *157*, 36–42. [CrossRef]
57. Caley, E.R. *Orichalcum and Related Ancient Alloys*; American Numismatic Society: New York, NY, USA, 1964.
58. Tolkien, T.; Wilkinson, H. *A Collector's Guide to Costume Jewelry Key Styles and How to Recognize Them*; Firefly Books: Willowdale, ON, Canada, 1997.
59. Moffat, T.P.; Stafford, G.R.; Hall, D.E. Pitting Corrosion of Electrodeposited Aluminum-Manganese Alloys. *J. Electrochem. Soc.* **1993**, *140*, 2779–2786. [CrossRef]
60. Sisko, M.; Pfaffli, I. *Fiber Atlas-Identification of Papermaking Fibers*; Springer: Espoo, Finland, 1995.
61. Carrillo, F.; Colom, X.; Suñol, J.J.; Saurina, J. Structural FTIR analysis and thermal characterisation of lyocell and viscose-type fibres. *Eur. Polym. J.* **2004**, *40*, 2229–2234. [CrossRef]
62. Gorassini, A.; Adami, G.; Calvini, P.; Giacomello, A. ATR-FTIR characterization of old pressure sensitive adhesive tapes in historic papers. *J. Cult. Herit.* **2016**, *21*, 775–785. [CrossRef]

- 
63. Hiroyuki, I. An Outline of Japanese Gold and Silver Production. *Wat on Earth*. University of Waterloo. 22 August 2002. Available online: <https://uwaterloo.ca/wat-on-earth/news/outline-japanese-gold-and-silver-production> (accessed on 15 July 2021).
  64. Kobata, A. The Production and Uses of Gold and Silver in Sixteenth-and Seventeenth-Century Japan. *Econ. Hist. Rev.* **1965**, *18*, 245–266. [[CrossRef](#)]
  65. Giumlia-Mair, A. Tin rich layers on ancient copper based objects. *Surf. Eng.* **2005**, *21*, 359–367. [[CrossRef](#)]